The ISME Journal, 2024, **18(1)**, wrae173
https://doi.org/10.1093/ismejo/wrae173
Advance access publication: 14 September 2024
Original Article

Oxidation of sulfur, hydrogen, and iron by metabolically versatile *Hydrogenovibrio* from deep sea hydrothermal vents

Katja Laufer-Meiser[1,*], Malik Alawi[2], Stefanie Böhnke[1], Claus-Henning Solterbeck[3], Jana Schloesser[3], Axel Schippers[4], Philipp Dirksen[2], Thomas Brüser[5], Susann Henkel[6], Janina Fuss[7], Mirjam Perner[1,*]

[1]Marine Geosystems, GEOMAR Helmholtz Centre for Ocean Research Kiel, Wischhofstraße 1-3, 24148 Kiel, Germany
[2]Bioinformatics Core, University Medical Center Hamburg-Eppendorf, Martinistrasse 51, 20246 Hamburg, Germany
[3]Institute for Materials and Surfaces, Kiel University of Applied Sciences, Grenzstrasse 3, 24149 Kiel, Germany
[4]Federal Institute for Geosciences and Natural Resources (BGR), Stilleweg 2, 30655 Hannover, Germany
[5]Institute of Microbiology, Leibniz Universität Hannover, Herrenhäuser Straße 2, 30419 Hannover, Germany
[6]Alfred Wegener Institute Helmholtz Centre for Polar and Marine Research, Am Handelshafen 12, 27570 Bremerhaven, Germany
[7]Institute of Clinical Molecular Biology ,Kiel University, Rosalind-Franklin-Straße 12, 24105 Kiel, Germany

[*]Corresponding author: Katja Laufer-Meiser, GEOMAR – Helmholtz Centre for Ocean Research Kiel, RD2 Marine Biogeochemistry, Marine Geosystems, Research Group Geomicrobiology, Wischhofstraße 1-3, Kiel 24148, Germany. Email: klaufer@geomar.de and Mirjam Perner, GEOMAR – Helmholtz Centre for Ocean Research Kiel, RD2 Marine Biogeochemistry, Marine Geosystems, Research Group Geomicrobiology, Wischhofstraße 1-3, Kiel 24148, Germany. Email: mperner@geomar.de

Abstract

Chemolithoautotrophic *Hydrogenovibrio* are ubiquitous and abundant at hydrothermal vents. They can oxidize sulfur, hydrogen, or iron, but none are known to use all three energy sources. This ability though would be advantageous in vents hallmarked by highly dynamic environmental conditions. We isolated three *Hydrogenovibrio* strains from vents along the Indian Ridge, which grow on all three electron donors. We present transcriptomic data from strains grown on iron, hydrogen, or thiosulfate with respective oxidation and autotrophic carbon dioxide (CO_2) fixation rates, RubisCO activity, SEM, and EDX. Maximum estimates of one strain's oxidation potential were 10, 24, and 952 mmol for iron, hydrogen, and thiosulfate oxidation and 0.3, 1, and 84 mmol CO_2 fixation, respectively, per vent per hour indicating their relevance for element cycling *in-situ*. Several genes were up- or downregulated depending on the inorganic electron donor provided. Although no known genes of iron-oxidation were detected, upregulated transcripts suggested iron-acquisition and so far unknown iron-oxidation-pathways.

Keywords: *Hydrogenovibrio*, iron oxidizer, hydrogen oxidizer, sulfur oxidizer, chemolithoautotrophy, autotrophic CO_2 fixation: Indian ridge, hydrothermal vent environment bacteria

Introduction

In deep-sea hydrothermal vent systems, hot and reduced hydrothermal fluids enriched in carbon dioxide (CO_2), hydrogen (H_2), methane, reduced sulfur (S) species, and metals (e.g., iron, Fe), rise from cracks in the basaltic ocean crust where seawater is circulating and transformed into hydrothermal fluids. They mix with entrained ambient, oxic, cold waters, creating thermal and chemical gradients along the fluid pathway [1]. In the mixing zone, intermediate inorganic S species like S^0, thiosulfate ($S_2O_3^{2-}$), and polysulfide can be found [2, 3]. This chemical disequilibrium can be exploited by chemolithotrophic microorganisms catalyzing the oxidation of these reduced substances to conserve energy that can be utilized for autotrophic CO_2 fixation [1, 4]. One group of chemolithoautotrophs that is often abundant in well mixed hydrothermal environments are *Hydrogenovibrio* spp. [5–9]. Members of this group were originally placed into the genus *Thiomicrospira* [10] and described as typical S-oxidizers capable of using H_2, hydrogen sulfide (H_2S), $S_2O_3^{2-}$, $[S_n(SO_3)_2]^{2-}$, and S^0 under aerobic or microaerobic conditions [7, 8, 11, 12]. Based on physiology, morphology, and phylogeny they were reclassified as *Hydrogenovibrio* [13].

Recent work showed that several *Hydrogenovibrio* spp. can harness energy from H_2 oxidation [5, 14]. The so far only strain capable of Fe(II) and $S_2O_3^{2-}$ oxidation, *Hydrogenovibrio* sp. SC-1, was isolated from a non-hydrothermal marine habitat by microbial traps positioned in Catalina Island off California, USA [15]. To our current knowledge, Fe(II) oxidation has not been tested for other *Hydrogenovibrio* spp. However, in incubation experiments with hydrothermal fluids to which Fe(II) was added, CO_2 fixation rates were highly stimulated, while the relative abundance of *Hydrogenovibrio/Thiomicrospira* increased from 15% in the environment to >50% in the incubations [6], highlighting that this metabolic potential is likely more common in this group than thought. Until today it has not been demonstrated that a member of this group can grow with all three electron donors (Fe(II), H_2, S). Such metabolic versatility would be highly beneficial, given the temporal and spatial dynamics existing in hydrothermal vent

Received: 11 April 2024. **Revised:** 22 July 2024. **Accepted:** 12 September 2024

environments and may explain why *Hydrogenovibrio* species are present at geographically distinct places with distinct vent chemistry [14, 16].

Here we report the isolation of three *Hydrogenovibrio* strains from three different vents along the Indian Ridge (IR). Members of the genus *Hydrogenovibrio* have previously been shown to dominate in hydrothermal vent communities of the South-West Indian Ridge (SWIR) [9, 17], and more recently a strain has been isolated from an active hydrothermal vent chimney at the SWIR that is capable of S and H_2 oxidation (*Hydrogenovibrio thermophilus* strain S5) [14]. We demonstrate that our isolates can oxidize Fe(II), H_2, and $S_2O_3^{2-}$, thereby gaining sufficient energy to synthesize biomass. We calculate the potential these strains have for element cycling in IR vents. Further, we link this physiological work with shifts in the transcriptomic data under the three incubation conditions and identify genes related to the different metabolisms.

Material and methods

Field sites and sampling

Hydrothermal vent fluid samples were collected during the BGR led INDEX 2019 cruise on RV Sonne SO-271 along the Central Indian Ridge (CIR) and South-East Indian Ridge (SEIR). Field sites, sampling, and chemical parameters of the hydrothermal fluids are described in detail by Adam et al. [17]. Fluid samples used for the isolation of the three strains were 040 KIPS C/D (F1, VF4, CIR), 083 KIPS A/B (F2, VF1, SEIR), 104 KIPS C/D (F3, VF2, SEIR) (for more details see Table S4).

Quantification of cell numbers

For cell counts, a subsample of the hydrothermal fluids was fixed with 4% formaldehyde) for 24 h at 4°C. The fixed cells were then concentrated on polycarbonate filters (type: Nucleopore, 0.2 μm pore size, Whatman, Buckinghamshire, United Kingdom), washed with sterile PBS and stored at −20°C. Filter sections were stained with DAPI (4′,6-Diamidin-2-phenylindol) and cells counted under an epifluorescence microscope.

Enrichment and isolation

Alongside the enrichment cultures that were described by Adam et al. [17], enrichments from the fluids 040 KIPS C/D, ROPOS 083 KIPS A/B, and 104 KIPS C/D were set up on ZVI (zero valent iron) plates under microoxic conditions to enrich for microaerophilic Fe(II)-oxidizers. The ZVI plates were prepared as previously described [18] with artificial seawater (ASW), N_2/CO_2 (80:20) as headspace and pH 6.8. Detailed information on the ZVI plates and medium composition can be found in the SI (Table S3). After the initial enrichment, cultures were subjected to dilution to extinction series for isolation. Growth was regularly checked by brightfield and fluorescence microscopy, where the cells were stained with LIVE/DEAD stain (BacLight, Invitrogen, Waltham, MS, USA). The purity of the culture was confirmed by microscopic examination and sequencing of the 16S rRNA gene. Strains 083 and 104 were deposited at the DSMZ under accession numbers DSM 117350 and DSM 117349. Strain 040 was physiologically very similar to strain 104 and therefore not deposited at the DSMZ.

DNA isolation and sequencing of the 16S rRNA gene

DNA was extracted with the NucleoSpin Soil kit (Macherey-Nagel, Düren, Germany) according to the manufacturer's instructions. The bacterial 16S rRNA gene was PCR amplified using the primers 27F/1492R [19] and sequenced by Sanger sequencing (Eurofins Genomics, Ebersberg, Germany). The phylogenetic tree of the strains and their closest relatives was constructed with MEGA X [20] based on the Maximum-likelihood method and Tamura-Nei model with 1000 bootstrap replications after multiple alignments using ClustalW [21].

Growth on various electron acceptors and donors

Growth was tested on FeS (in gradient tubes) and $FeCl_2$ under microoxic conditions, $FeCl_2$ and NO_3^-, H_2S and NO_3^-, H_2S, and O_2 (in gradient tubes), $S_2O_3^{2-}$ and NO_3^-, and $S_2O_3^{2-}$ and O_2.

Growth on Fe(II) and quantification of Fe(II) oxidation rates

To confirm growth on Fe(II) cultures were also grown in gradient tubes with an FeS plug in the bottom and in liquid ASW medium containing $FeCl_2$. Gradient tubes contained gel-stabilized ASW with a bottom layer containing 1% (wt/vol) agarose with a 1:1 mixture of FeS and ASW medium overlain by ASW medium with 0.15% (wt/vol) agarose and air in the headspace [22, 23]. In gradient tubes, cultures were inoculated vertically over the whole length of the tube. Cultures in ASW with $FeCl_2$ were grown in 100 ml serum vials containing 50 ml ASW, 500 μM $FeCl_2$ with a headspace of N_2/CO_2 (80:20) to which sterile air was added to reach an oxygen concentration of ∼1%. The headspace was flushed daily with N_2/CO_2, and afterwards 500 μM $FeCl_2$ and fresh sterile air (1% final O_2 concentration) was added.

Fe(II) oxidation rates were determined in cultures grown in ASW with $FeCl_2$. Each day samples from the culture were taken and fixed with 1 M HCl (final concentration). At the same time, a sample for cell counting was taken and fixed with 4% formaldehyde. The concentration of Fe(II) and total Fe was measured photometrically with the Ferrozine Assay [24], and for total Fe measurements all Fe(III) was reduced to Fe(II) with hydroxylamine hydrochloride. Fe(III) concentrations were calculated by subtracting Fe(II) from total Fe. Uninoculated replicates were taken as abiotic controls. Fe(II) oxidation rates were calculated from the difference between the biotic and abiotic incubations. Total cell counts were performed as described above.

Growth on H_2 and quantification of H_2 oxidation rates

Cultures growing on H_2 were cultivated in 16 ml Hungate tubes, containing MJ medium (detailed composition Table S3) with a $H_2/CO_2/O_2$ (79:20:1) headspace. Resazurin was added as redox indicator and the cultures were flushed with $H_2/CO_2/O_2$ (79:20:1) regularly once the medium became clear.

For quantification of H_2-consumption rates, cultures were grown in 100 ml serum vials with 50 ml MJ medium and a $H_2/N_2/CO_2/O_2$ (2:77:20:1) headspace. H_2 concentrations in the headspace were measured with a Trace GC Ultra gas chromatograph (ThermoFisher Scientific, Waltham, MA, USA), using a ShinCarbon ST 100/120 column (Restek Corporation, Bellefonte, PA, USA) and a Pulsed Discharge Detector (Vici Valco Instruments, Houston, TX, USA) as previously described [5]. Uninoculated replicates were used as controls. Cell counts were performed as described above.

Growth on $S_2O_3^{2-}$ and quantification of $S_2O_3^{2-}$ oxidation rates

Cultures growing on $S_2O_3^{2-}$ were cultivated in 100 ml serum flasks containing 50 ml of T-ASW medium with 40 mM $S_2O_3^{2-}$ (detailed composition Table S3) and sterile air in the headspace. Cultures were also grown on T-ASW plates, which were prepared with T-ASW medium and 1.5% agar. For quantification of $S_2O_3^{2-}$oxidation rates, samples were taken over time and the

$S_2O_3^{2-}$ concentration was measured via high-performance liquid chromatography (HPLC) as previously described [25, 26]. Uninoculated replicates were used as controls. Cell numbers were quantified as described above.

Quantification of ^{14}C-HCO_3^- incorporation rates during Fe(II), H_2, and $S_2O_3^{2-}$ oxidation

For quantification of ^{14}C-HCO_3^- incorporation rates for strain 104 with the three different substrates, cultures were set up as described above for the rate measurements. The following treatments were prepared in triplicates for each of the electron donors in a ^{14}C version and a no radioactivity version: (i) control without cells with electron donor, (ii) control with cells without electron donor, and (iii) a treatment with cells with electron donor. The ^{14}C treatments were initially incubated and sampled in parallel with the other treatments and after 6 h for $FeCl_2$, 8 h for H_2 and 24 h for $S_2O_3^{2-}$ 1 μCi of ^{14}C-$NaHCO_{3-}$ (specific activity of 50–60 mCi mmol^{-1}) was injected to the vials and incubated for 18, 17, and 24 h for $FeCl_2$, H_2, and $S_2O_3^{2-}$, respectively. The ^{14}C incubation was stopped by adding formaldehyde (final concentration 4% (v/v)). At the same time, the non-^{14}C parallel treatments were continuously sampled to determine the consumption of $FeCl_2$, H_2 and $S_2O_3^{2-}$, and cell numbers during the ^{14}C incubation.

For quantification of ^{14}C incorporation, samples for DIC concentration measurements were taken before tracer addition, and fixed with $HgCl_3$. For cultures grown on H_2 and $FeCl_2$ DIC was quantified with a QuAAtro four-channel flow injection Analyzer (Seal Analytical) and the respective standard QuAAtro method (Q-067-05 Rev.1). For cultures grown on $S_2O_3^{2-}$ DIC was quantified by flow-injection using a conductivity method with 30 mM HCl as carrier and 5 mM NaOH as receiver.

Just before the ^{14}C incubation was stopped, 100 μl of supernatant from each vial was added to a scintillation vial containing scintillation cocktail (Ultima Gold XR, PerkinElmer) to determine the total radioactivity in the culture by liquid scintillation counting (TriCarb 291001, PerkinElmer). The remaining culture was concentrated on polycarbonate filters (pore size 0.22 μm), washed with sterile PBS solution, and leftover bicarbonate was removed by acid fuming for 24 h with 2 M HCl in a desiccator. The $FeCl_2$ filters were additionally treated with oxalic acid/ammonium oxalate solution (100 mM/80 mM) and Fe(II)-EDAS (100 mM) while the filter was still mounted on the filtration tower to dissolve Fe-minerals, including siderite, and washed with sterile PBS again before acid fuming. The filters were added to scintillation vials, scintillation cocktail was added and the radioactivity quantified by liquid scintillation counting. The rate of C-fixation per ml culture per hour was calculated as described previously [27].

Quantification of RubisCO enzyme activity

Specific RubisCO activity was measured with an HPLC based enzyme assay as previously described [28, 29]. A 1 l batch of *Hydrogenovibrio* strain 104 was cultured under the same conditions as outlined above for the rate measurements with H_2. Crude extracts were prepared using a French pressure cell press (Thermo Spectronic) (for detailed information see SI). RubisCO activity was measured at 25°C in RubisCO assay buffer [100 mM Tris–HCl (pH 7.8), 10 mM $MgCl_2$, 1 mM EDTA, 25 mM $NaHCO_3$, and 1 mM DTT] with 0.2 mg μl^{-1} protein crude extract and 10 mM ribulose-1,5-bisphosphate (RuBP). The consumption of RuBP was quantified using the LaChrom Elite HPLC system (Hitachi, Tokio, Japan) with a Lichrospher 100 RP 18e column (VWR International GmbH, Darmstadt, Germany) (for further information see SI).

Transcriptomic analyses under different growth conditions

For transcriptomic analyses, strain 104 was grown with H_2, $S_2O_3^{2-}$, and $FeCl_2$ as described above (45 × 50 ml). After harvesting the cultures in the late exponential phase by centrifugation, RNA was extracted using the Marchery and Nagel NucleoBond RNA soil mini kit (Düren, Germany) according to manufacturer's protocol but with Chloroform:Isoamylalcohol (24:1) instead of Phenol:Chloroform:Isoamylalcohol (25:24:1). Residual genomic DNA was removed using the RapidOut DNA Removal Kit as specified by the manufacturer (ThermoFisher Scientific) and the absence of genomic DNA was verified via PCR. Library preparation for transcriptome sequencing was done with the Stranded Total RNA Prep kit with the Ribo-Zero plus rRNA depletion kit (Illumina, San Diego, USA) according to manufacturer's protocol. Sequencing was performed on a NovaSeq 6000 System (2 × 150 bp; Illumina) with the NovaSeq 6000 SP Reagent Kit v1.5 and NovaSeq XP 2-Lane Kit v1.5.

Sequence reads were processed with FASTP (v0.23.2) [X] to remove artificial sequences originating from adapters, low quality sequences (more than 40% of bases below a phread quality score below 15), and to correct bases in the overlap regions of the forward and reverse reads of each read pair. Reads were than aligned to the NCBI RefSeq assembly GCF_003991075.1 (strain S5, which had based on 16S rRNA gene 100% sequence similarity to our strain) with BWA MEM (v0.7.17-r1188). Samtools (v1.16) was used for sorting the alignments and featureCounts from the Subread package (v.2.0.6) was employed to obtain counts per gene based on the genomic coordinates provided with the aforementioned RefSeq assembly. Normalization and differential expression analysis were carried out with DESeq2 (v.1.40.1). Although the selection of the reference strain can have a significant impact on the results, we also carried out a complementary analysis without using any reference strain. For this, we performed a transcriptome assembly with Trinity (v2.15.1) and then annotated the assembled transcripts with Prokka (v1.14.6). By this approach we could also not detect any of the known genes involved in Fe oxidation (e.g., cyc2) as summarized elsewhere [30].

Results

Isolation of three *Hydrogenovibrio* strains from IR vent systems

Hydrothermal fluids from VF4 (CIR), VF1 (SEIR), and VF2 (SEIR) [17] were used for enrichment on ZVI-plates. Cells were uniform and were mostly attached to Fe-minerals, which appeared as bulbous structures. EDS analysis confirmed that the bulbous structures consist of elemental Fe (Fig. 1) and XRD analysis of the products confirmed existence of crystalline α-Fe. 16S rRNA gene sequence comparison showed that the strains were most closely related to *Hydrogenovibrio thermophilus* strains JR-2 and S5 (Fig. 2) with 99.9, 100, and 100% sequence similarity for strain 040, 083, and 104, respectively. More information can be found in SI.

Growth of strains and quantification of electron donor oxidation and C-fixation rates

Growth was observed on FeS gradient tubes, $FeCl_2$ and O_2 (microoxic, 1% O_2), H_2 and O_2 (microoxic, 1% O_2), and S_2O_3 [2] and O_2 (fully oxic) (Table 1). On H_2 (MJ medium) and $S_2O_3^{2-}$ (T-ASW medium), growth was confirmed by color change of the medium (blue to pink to colorless for MJ and red to yellow for

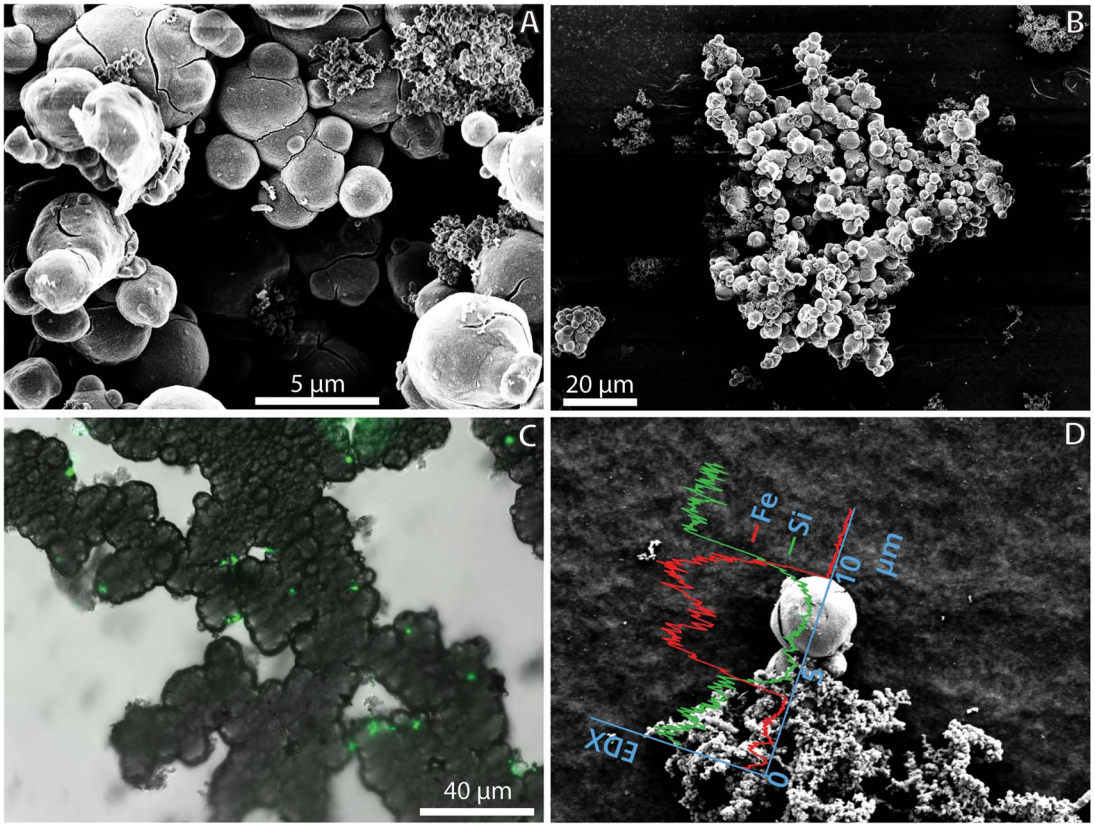

Fig. 1. Microscopy, and EDX of culture 104 grown on ZVI. (A and B) SEM images. In a cells attached to the bulbous mineral structures can be seen. (C) Overlay of brightfield and fluorescence microscopy. The Fe-minerals appear dark in brightfield microscopy, the cells are stained with LIVE/DEAD stain and visible in fluorescence microscopy. D: SEM image with overlain EDX spectrum measured along the x-axis of the EDX graph.

Table 1. Effect of redox substrates on growth of strains 040, 083, and 104.

	e^- acceptor	
e^- donor	**O_2**	**NO_3^-**
ZVI	+	n.d.
$FeCl_2$	+	–
FeS gradient	+	n.d.
H_2	+	n.d.
H_2S	–	–
$S_2O_3^{2-}$	+	n.d.

n.d. = not determined

T-ASW) as well as by microscopy. On T-ASW, growth was also visible from the formation of a white precipitate, likely ZVS (zero valent S).

Microbial Fe(II), H_2, and $S_2O_3^{2-}$ oxidation rates

Cell numbers in the Fe(II)-amended cultures increased on average 4.8-, 3.9-, and 3.0-fold within 3 days for culture 040, 083, and 104. This is lower than what was reported for SC-1, for which cell numbers increased by two orders of magnitude within a week [15]. Maximum Fe(II) oxidation rates were 0.016 (± 0.002), 0.008 (± 0.004), and 0.010 (± 0.002) μmol Fe(II) ml $^{-1}$ h^{-1} for culture 040, 083, and 104, respectively (± are SD). Cell-specific rates were 1.6, 0.9, and 1.7 fmol Fe(II) $cell^{-1}$ h^{-1} for culture 040, 083, and 104, respectively. Cultures 040 and 104 completely oxidized all H_2 in the headspace within 48 h; culture 083 was slower but also completely oxidized all H_2 available within 96 h (Fig. 3). Maximum H_2 oxidation rates were 145.2 (± 18.2), 75.4 (±3.0), and 140.3 (±6.2) nmol ml^{-1} h^{-1} for culture 040, 083, and 104, respectively. Per cell, the rates were 1.8, 9.2, and 1.7 fmol H_2 $cell^{-1}$ h^{-1}. This is very similar to what is reported for strain SP-41 (1.47–6.10 fmol H_2 $cell^{-1}$ h^{-1}) [5]. In all cultures $S_2O_3^{2-}$ was completely oxidized within 120 h (Fig. 3). Maximum $S_2O_3^{2-}$ oxidation rates were 1.16 (± 0.026), 1.05 (± 0.05), and 2.06 (± 0.014) μmol $S_2O_3^{2-}$ ml^{-1} h^{-1} for culture 040, 083, and 104, respectively. Cell specific rates were 53.6, 190.8, and 262.4 fmol $S_2O_3^{2-}$ $cell^{-1}$ h^{-1} for culture 040, 083, and 104, respectively. The oxidation rates are similar to those reported for *Hydrogenovibrio thermophilus* S5, which oxidized maximal 1.04 μmol $S_2O_3^{2-}$ ml^{-1} h^{-1} [14].

Autotrophic CO_2 fixation rates

Autotrophic CO_2 fixation rates were determined for strain 104 by measuring ^{14}C-HCO_3^- incorporation during growth on $FeCl_2$, H_2, and $S_2O_3^{2-}$. The highest rates of ^{14}C-HCO_3^- fixation (per ml culture and per cell) were found when the culture was grown with $S_2O_3^{2-}$, whereas the lowest C-fixation rates were found when the culture was grown with Fe(II) as electron donor (Table 1). ^{14}C incorporation measurements with hydrothermal fluids conducted in other studies reported significantly lower cell-specific rates in the range of 0.0001–0.1 fmol $cell^{-1}$ h^{-1} [31, 32]. In a previous study [6] rates quantified in incubation experiments with hydrothermal fluids to which Fe(II) was added were in the range of 4×10^{-7} to 20×10^{-7} mmol C ml^{-1} h^{-1}. The rates in mmol C ml^{-1} h^{-1} we quantified for our strain with Fe(II) were in the lower range of this. Autotrophic CO_2 fixation in *Hydrogenovibrio* is operated by the Calvin-Benson-Bassham cycle with RubisCO as the key

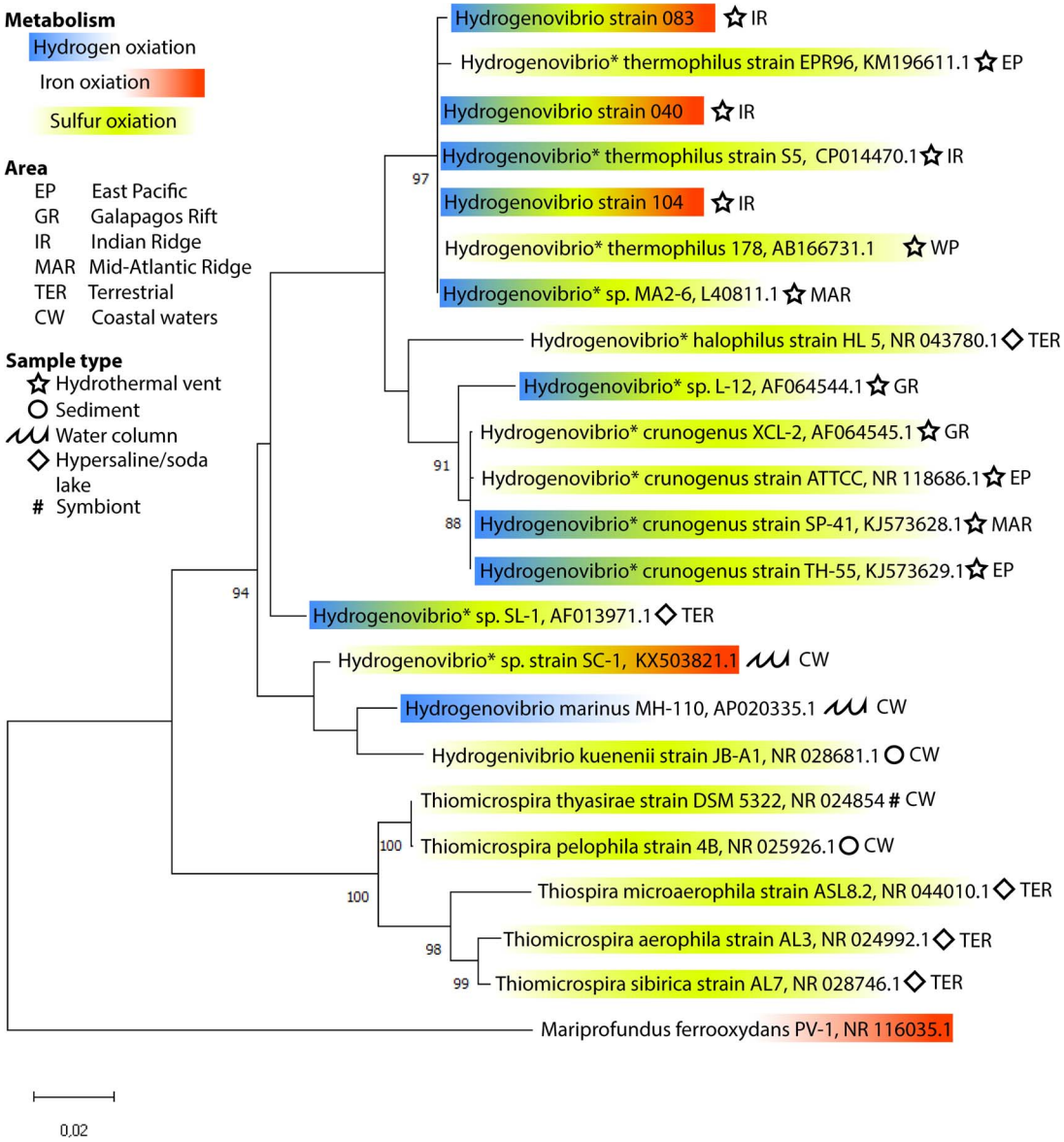

Fig. 2. Phylogenetic tree. Phylogenetic tree based on 16S rRNA gene sequences, showing the phylogenetic relationship of the three isolates and closely related strains. * indicate which strains have been reclassified from *Thiomicrospira* to *Hydrogenovibrio* [13]. Colors indicate experimentally verified metabolic capabilities of the strains as indicated in the legend. Bootstrap values are only displayed if above 80%. The scale bar represents the expected number of changes per nucleotide position. *M. ferrooxydans* is added as an outgroup.

carboxylating enzyme [14, 33]. The specific RubisCO activity of *Hydrogenovibrio* strain 104 grown under H_2:CO_2:O_2 (79:20:1) atmosphere was 41.5 ± 7 nmol RuBP per min and mg of protein crude extracts in the exponential growth phase which is 3.0 to 9.9 times lower then what has been measured for other *Hydrogenovibrio* isolates (Table 2).

This significant difference in RubisCO activities might reflect that RubisCO enzymes of strain 104 expressed under the given cultivation conditions actually have comparatively poor catalytic properties. However, the apparently reduced RubisCO activity could just as well be caused by methodological biases in the quantification of RubisCO activities (e.g., ^{14}C incorporation versus HPLC assay, see Table 2). The transcriptomic data, though, suggest that genes associated with the carboxysome operon are down-regulated in H_2-treated cultures, which could also explain the rather low RubisCO activity (more information follow in section below).

Transcriptomic analyses under different growth conditions

Transcriptomic analyses were performed for strain 104 under the three growth conditions, namely with Fe(II), H_2, and $S_2O_3^{2-}$ and revealed significant differences in the expression patterns (Fig. S6). Whereas over 500 genes are differentially expressed (FDR ≤ 0.05 and $|\log_2 FC| \geq 1$) when comparing $S_2O_3^{2-}$ against H_2, about twice as many are observed in comparisons including $FeCl_2$ (Table S4). Here we present the most important findings regarding Fe(II), H_2, and $S_2O_3^{2-}$ oxidation and C-fixation. A more detailed description of the results from the transcriptome analysis can be found in the SI.

Transcriptomic shifts of genes related to energy metabolism.

There are only two known genes involved in neutrophilic microaerophilic Fe(II) oxidation (*cyc2* and *mtoAB*) [30]. Neither is

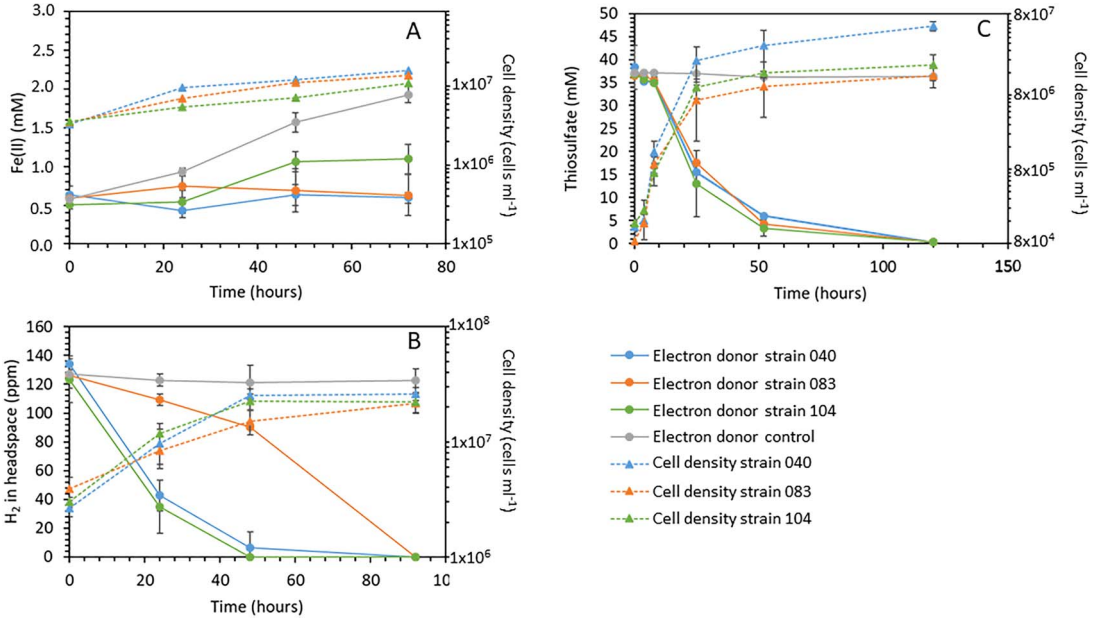

Fig. 3. Rates of electron donor oxidation and cell numbers over time. Concentrations of electron donors and numbers of cells over time for all three cultures grown on (A) Fe(II), (B) H_2^-, and (C) $S_2O_3^{2-}$. Symbols are the mean (n = 3), error bars show standard deviation.

Table 2. CO_2 fixation rates for strain 104 and specific RubisCO activities for strain 104 and other *Hydrogenovibrio* species.

CO_2 fixation rates	**mmol C-fixation ml^{-1} h^{-1}**	**fmol C-fixation $cell^{-1}$ h^{-1}**	
$S_2O_3^{2-}$ oxidation strain 104	$1.26x10^{-4} \pm 9.31x10^{-6}$	23.30 ± 1.72	
H_2 oxidation strain 104	$5.16x10^{-6} \pm 3.27x10^{-7}$	0.29 ± 0.019	
Fe(II) oxidation strain 104	$7.77x10^{-7} \pm 7.52x10^{-7}$	0.09 ± 0.082	
RubisCO activities	**nmol RuBP min^{-1} mg^{-1}**	**reference**	**method**
H. crunogenus TH-55	126 ± 8	[28]	HPLC
H. crunogenus XCL-2	410 ± 20	[37]	^{14}C incorporation
H. thermophilus I78	222 ± 40	[76]	HPLC
Hydrogenovibrio 104	41 ± 7	this study	HPLC

included in the reference annotation. A number of genes encoding redox proteins (oxidoreductases) were induced with Fe(II) versus $S_2O_3^{2-}$ that likely relate to electron transport from iron to oxygen, most prominently genes of the sarcosine oxidase subunit delta (Fig. 4). A genetic association with formyltetrahydrofolate deformylase (*purU*) and a high induction of the system points to a highly important interrelation of C1-metabolism and sarcosine oxidase. The physiological function of this sarcosine oxidase and the importance of it specifically during growth with Fe(II) would be an interesting aspect for future research. Genes involved in Fe transport and storage were upregulated during growth on Fe(II), most prominently a TonB-dependent receptor. In Gram-negative bacteria the TonB-dependent receptor mediates the transport of siderophores into the periplasm (together with *ExbB* and *ExbD*, which are also in the transcriptome but were not significantly upregulated with Fe(II) (Fig. S4) [34–36]. Moreover, a Pirin family protein, 2Fe-2S iron–S cluster binding protein, and some hypothetical proteins were upregulated. As these are specifically induced under Fe(II)-oxidizing conditions, these enzymes likely are somehow involved in Fe oxidation or the subsequent electron transport pathway in this organism.

Hydrogenases (H_2-converting enzymes) were detected on the genome of *Hydrogenovibrio* already in 2006 [37], but H_2 oxidation was experimentally verified only ~10 years later [5, 38]. *Hydrogenovibrio* species have been shown to possess [NiFe]-hydrogenases of group 1 (*hyaAB*) and group 2b (*hupUV*) [5, 14, 38]. Hydrogenase-related genes were upregulated in cells grown on H_2 relative to those on $S_2O_3^{2-}$ (Fig. 4). Unexpectedly, for cells grown with Fe(II), some hydrogenase-related genes were upregulated relative to those from H_2 amended incubations.

Hydrogenovibrio species rely on the Sox enzyme system and the sulfide:quinone reductase (Sqr) for $S_2O_3^{2-}$ oxidation [14, 37]. Strain 104 has an incomplete Sox pathway, *soxB*, *soxD,* and *sqr* genes are missing. The incomplete pathway results in the intra- or extracellular accumulation of ZVS [39, 40]. Genes *soxZ*, *soxC*, *soxY,* and *soxX* were upregulated in the $S_2O_3^{2-}$ vs. H_2 comparison, whereas *soxA* was slightly downregulated (Fig. 4). When the strain was grown with Fe(II) and H_2, generally *sox* genes were downregulated and genes needed for assimilatory sulfate reduction (*cysD* and *cysN*, APS reductase, *cysI, cysG*) were upregulated, showing that the strain used sulfate, the sole S-source in these media, for assimilation.

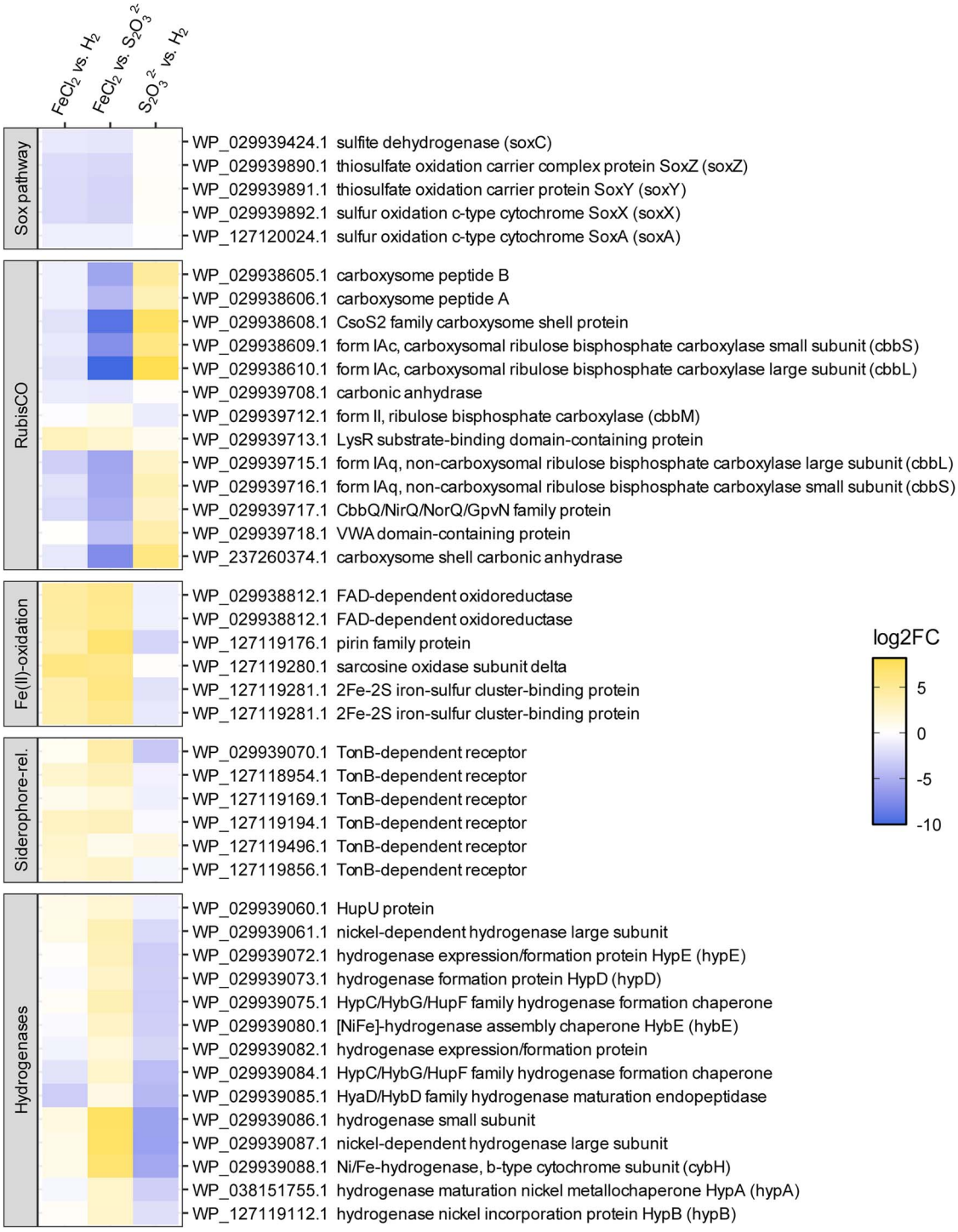

Fig. 4. Transcription of selected genes related to metabolic sulfur, iron, or hydrogen oxidation in *Hydrogenovibrio*. Each gene is differentially regulated in at least one of the three comparisons. An extended heatmap can be found in Fig. S4.

Transcriptomic shifts of genes related to autotrophic CO_2-fixation

Transcriptomic data indicate that strain 104 features multiple RubisCO enzymes, which may allow to facilitate CO_2 fixation at a variety of CO_2 and O_2 exposures, as has been shown for other *Hydrogenovibrio* strains before [41]. A total of three RubisCOs types were found to be transcribed in *Hydrogenovibrio* strain 104, namely (i) a carboxysomal form IA (IAc), (ii) a non-carboxysomal form IA (IAq), and (iii) a form II RubisCO. Both, form IAc and IAq RubisCO structural genes (*cbbLS*) were markedly upregulated when *Hydrogenovibrio* strain 104 grew with $S_2O_3^{2-}$ (Fig. 4), which coincides with the enhanced growth observed under this treatment (Fig. 3). RubisCO form II is compared to RubisCO form I the faster catalyst, which, however, comes at the expense of a lower specificity towards CO_2 and results in lower tolerances to oxygen [42]. Using *Hydrogenovibrio marinus* it was demonstrated that the three RubisCO operons are regulated in response to CO_2 concentration, with elevated CO_2 levels (<2%) promoting CbbM

synthesis [43]. The down regulation of the form II RubisCO structural gene *cbbM* in the $S_2O_3^{2-}$ treatment, performed under fully oxic conditions and atmospheric CO_2 levels is therefore plausible, as is its significant upregulation in the low-O_2 but high-CO_2 treatments, i.e., cultures grown with H_2 and $FeCl_2$ in a 20:80 CO_2:N_2 atmosphere with 1% O_2. However, the non-carboxysomal form IAq is significantly downregulated when comparing H_2 and $FeCl_2$ treatments, although the starting O_2 and CO_2 levels are identical in both experiments, suggesting that the O_2 and CO_2 levels are not the only factor determining the expression of RubisCO, but that available electron donors are directly or indirectly also of relevance.

The carboxysomal RubisCO form IAc of strain 104 is arranged in a carboxysome operon together with the carboxysome shell proteins and a carboxysomal carbonic anhydrase. Thus, *Hydrogenovibrio* strain 104, like other *Hydrogenovibrio* species, possesses a carbon concentrating mechanism (CCM) that facilitates the active uptake of dissolved inorganic carbon to generate up to 100-fold increased intracellular versus extracellular concentrations [44, 45]. Therefore it is reasonable that the genes related to CCM (carbonic anhydrases and carboxysomes) were highly upregulated when strain 104 grew with $S_2O_3^{2-}$ under atmospheric i.e., comparatively low CO_2 concentrations, versus $FeCl_2$- and H_2-treated cultures growing under high CO_2 levels, i.e., with a CO_2:N_2 headspace of 20:80 (Fig. 4). Additional information on RubisCO associated genes (*cbbQO* and *lysR*) can be found in the SI.

Discussion

We describe three newly isolated strains of *Hydrogenovibrio* from hydrothermal vents of the IR, able to grow autotrophically by Fe(II), H_2, and $S_2O_3^{2-}$ oxidation. This study highlights the metabolic flexibility of *Hydrogenovibrio* providing a competitive advantage over other organisms to thrive in various vent environments.

All fluids from which the enrichments originate contained H_2S (<10–60 μM) and Fe(II) (1.3–45 μM) [17]. High H_2 concentrations have been measured in fluids of the Kairei vent field, located on the CIR, and previously H_2 oxidizers have been isolated or enriched from the IR [14, 17, 46]. Given that in the environment they are exposed to various electron donors, it is beneficial if microorganisms can switch between different metabolisms or simultaneously use them. On the ZVI plates that were used for isolation of the strains, Fe(II) and H_2 is available simultaneously as H_2 is produced from the reduction of H_2O by ZVI during the hydrogen evolution reaction (HER) [47], for more information see SI. The production of H_2 per ZVI oxidized during HER is quite significant with an overall stoichiometry between 1:1 to 4:3 [47]. That the strains can also grow on $FeCl_2$ and in gradient tubes with FeS in the bottom plug shows that they do not depend on H_2 for growth but can grow autotrophically on Fe(II) alone. It is yet to be investigated which electron donor they prefer or if they can make use of them simultaneously, as it was shown previously for the Fe(II)- and H_2-oxidizing *Ghiorsea bivora* [48], which had a growth benefit when both electron donors were present simultaneously. When strain 104 was growing on $FeCl_2$ we found that hydrogenases were amongst the genes with the highest log2-fold change compared to cells grown on $S_2O_3^{2-}$. This is an indication that the strain may be using both metabolisms simultaneously in the environment. ZVI plates, which were used for isolation, would provide an advantage for organisms being able to use H_2 and Fe(II) simultaneously and therefore likely specifically select for organisms with this ability.

Most microaerophilic Fe(II)-oxidizers are described to produce twisted stalks or sheaths as characteristic Fe(III)-mineral structures [49–51]. This is different for our strains, they produce "coral-like" structures consisting of bulbous Fe(III)-minerals with ~1–6 μm in diameter (Fig. 1). These structures appear very different from Fe(III) that precipitated in abiotic controls and are similar to what is reported for *Ghiorsea bivora* [48], a Zetaproteobacterium that is also capable of Fe(II) and H_2 oxidation, and *Hydrogenovibrio* sp. SC-1, the only other known *Hydrogenovibrio* capable of Fe(II) oxidation [15]. For *Ghiorsea* it was shown that it produces soluble exometabolites. These exometabolites are responsible for the Fe(III)-mineral formation outside the cell, that is different from abiotic mineral formation [52]. We could not find any known genes for Fe(II) oxidation in the transcriptome, therefore we conclude that, as previously suggested for SC-1 [15], the organism uses another Fe(II) oxidation pathway as indicated by Fe(III)-minerals being different from those generated by other Fe(II)-oxidizers. The genome of SC-1 was also sequenced and no known genes for Fe oxidation can be found in the genome [53].

When the strain 104 was grown on $FeCl_2$, hydrogenases were upregulated compared to S_2O_3 [2]. Five of thirteen observed hydrogenase-related genes were significantly higher expressed with $FeCl_2$ than in H_2, whereas two were significantly less expressed (Fig. 4). However, the latter two are other hydrogenases than the ones important for H_2 oxidation as seen from the comparison of H_2 and $S_2O_3^{2-}$, as they are also downregulated in this comparison.

It could be that hydrogenases are upregulated with $FeCl_2$ as the strain potentially uses Fe(II) and H_2 simultaneously. However, under the conditions that the Fe(II) culture was grown for the transcriptomic analyses, there is no H_2 available. Another reason for the upregulation could be that hydrogenases themselves are somehow involved in Fe(II) oxidation. This hypothesis would require further research though. Another interesting aspect is the upregulation of TonB in the culture grown on Fe(II). One possibility for the upregulation of genes related to siderophores in our strain could be that they are involved in the formation of the Fe(III) mineral structures, similar to the soluble exometabolites that are involved in Fe(III) mineral formation in *Ghiorsea* [52]. Siderophores have been found to be abundant and diverse in hydrothermal plumes [54]. They are important in keeping Fe in solution and thereby impact cycling and transport of iron in the ocean [55]. Whereas TonB can also be involved in the transport of carbohydrates [56], especially in venting regions where carbohydrates are abundant, such as the Guaymas Basin [57]. A study that investigated microbial genes involved in Fe uptake in hydrothermal plumes in the Guaymas Basin found that TonB was amongst the most abundant genes in the whole plume metatranscriptome [58] and the authors link that to Fe transport. That our strain has the potential to be involved in siderophore production/export highlights the environmental importance that Fe-oxidizing microbes such as *Hydrogenovibrio* might have.

Thermodynamically, thiosulfate is with −762 kJ/mol $S_2O_3^{2-}$ oxidized the most favorable of the investigated electron donors [59]. Hydrogen yields −237 kJ/mol H_2 [60] and microaerophilic Fe(II) oxidation only about −90 kJ/ mol Fe oxidized [61]. Results from the ^{14}C-HCO_3^- incorporation experiments show that the strain can grow autotrophically with all three tested electron donors. C-fixation rates with $S_2O_3^{2-}$ were much higher compared to H_2 and Fe(II), consistent with much higher cell growth and the high upregulation of RubisCO with $S_2O_3^{2-}$. Based on our measurements for C-fixation and concurrent substrate utilization, for each mole of C-fixed ca. 16, 23, and 35 moles of substrate had

to be oxidized for $S_2O_3^{2-}$, H_2, and Fe(II), respectively. The ratios of substrate oxidized per C-fixed in other autotrophic organisms range from 2:1 to 5:1 for aerobic sulfide oxidizers [62–65], 10:1 for ammonium oxidizers [66, 67], and 25:1 to 80:1 for nitrite oxidizers [68]. Considering that 4 mol electrons are needed for each mol of C-fixation, this means that ~7, 9, and 11% of the electrons transferred from the substrate went into C-fixation (for C-reduction) and the remaining electrons were used for energy generation. This agrees relatively well with previous reports that ~10–20% of the electrons are used for biomass synthesis [63, 69–71]. The values for oxidized Fe(II) per fixed CO_2 that we found for Fe(II)-oxidizing conditions are slightly lower than what was estimated previously for other neutrophilic microaerophilic Fe(II) oxidizers, for which values of 43 to 70 mol oxidized Fe(II) per mol of fixed CO_2 were suggested [72, 73]. The rates of CO_2-fixation were much higher for $S_2O_3^{2-}$compared to $FeCl_2$ and H_2, likewise the increase in cell numbers was much faster. It will have to be elucidated in the future, which is the favored electron donor in the environment where the strains were isolated from.

In the environmental samples used for isolation of our new strains, we found that *Hydrogenovibrio/Thiomicrospira* had a relative abundance of up to 6% [17]. For the fluid from which strain 104 was isolated we counted 3.44×10^6 cells ml^{-1}. This means that we potentially have up to 2.064×10^5 *Hydrogenovibrio* cells per ml of hydrothermal fluid. Assuming that all these cells consume either Fe(II), H_2, or $S_2O_3^{2-}$ at the rate measured for the isolates, we could find rates of C-fixation of 1.75×10^{-8}, 6.04×10^{-8}, and 4.8×10^{-6} mmol C ml^{-1} h^{-1}, respectively. Unfortunately, we do not have flow rates for the vents from which the samples originate. Based on literature, we assume rates for low-temperature diffuse vents between 116–17 580 l h^{-1} [74, 75]. Based on these numbers and the rates we measured with the cultures, between 71–10 777, 159–24 109, and 6282–952 183 μmol Fe(II), H_2, and $S_2O_3^{2-}$ could become oxidized per vent-site per hour, respectively. For C-fixation we calculated that during Fe(II), H_2, and $S_2O_3^{2-}$ oxidation by *Hydrogenovibrio* between 2–308, 7–1061, and 557–84 420 μmol C could be fixed per vent site and hour, respectively. These rates are potential rates that can be reached by a pure culture under ideal conditions. Thus, they are likely overestimates of what can be reached in the environment and many assumptions go into this calculation. The details of the calculation can be found in the SI (Table S5). Comparisons of the cell-specific ^{14}C fixation rates from our strain (Table 2) and rates determined in hydrothermal fluids, which were in the range of 0.0001–0.1 fmol $cell^{-1}$ h^{-1} [31, 32], show that our rates are high. However, in another study ^{14}C fixation rates with Fe(II) in hydrothermal fluids have been in the same range [6] (4×10^{-7} to 20×10^{-7} mmol C ml^{-1} h^{-1}, Table 2). Even though our estimates are rough, the calculations demonstrate that *Hydrogenovibrio* potentially substantially contributes to C, S, Fe, and H_2 cycling at these vents.

The metabolic versatility of the isolated strains highlight that *Hydrogenovibrio* species do not only play an important role in S and carbon cycling, but are also important in H_2 and iron cycling. Because no known genes for Fe(II) oxidation were found, we conclude that the strain uses a yet unknown pathway for Fe(II) oxidation. The metabolic versatility makes these strains good candidates for studying new Fe oxidation genes and mechanisms.

Acknowledgements

We thank the captain and crews of R/V Sonne as well as the ROV ROPOS for the excellent help with the retrieval of our deep-sea vent samples. Gabriele Schüssler, Jannes Hoffmann and Ronny Baaske are acknowledged for technical assistance and help with maintaining the cultures. We thank Ingrid Dohrmann for DIC measurements. The Institute of Clinical Molecular Biology (IKMB) at the University of Kiel is acknowledged for sequencing of the transcriptomes.

Author contributions

MP planned the study and secured funding. KLM collected samples, performed enrichment, isolation, cultivation of the strains, and physiological and ^{14}C incorporation experiments. MP and KLM evaluated data and wrote the manuscript. MA evaluated the transcriptomic data. SB quantified RubisCO activity, isolated RNA for the transcriptome sequencing and evaluated data. PD evaluated and visualized transcriptomic data. CHS and JS performed SEM and XRD analysis and evaluated the data. AS performed thiosulfate measurements and evaluated data. TB helped with the evaluation and discussion of transcriptomic data. SH supervised DIC measurements. JF performed transcriptome sequencing. All authors contributed to and revised the manuscript.

Supplementary material

Supplementary material is available at *The ISME Journal* online.

Conflicts of interest

The authors declare no competing interests.

Funding

The samples were recovered during a cruise within the exploration program INDEX by BGR. We thank the BGR for funding this study.

Data availability

Sequence data for the transcriptomes reported in this publication have been submitted to the European Nucleotide Archive. They are publicly available under accession PRJEB71696. The 16S rRNA gene sequences of all three strains were deposited under GenBank accession numbers PP083208, PP083209, and PP083210.

References

1. Jannasch HW, Mottl MJ. Geomicrobiology of deep-sea hydrothermal vents. *Science* 1985;**29**:717–25.
2. Gartman A, Yücel M, Madison AS *et al.* Sulfide oxidation across diffuse flow zones of hydrothermal vents. *Aquat Geochem* 2011;**17**:583–601. https://doi.org/10.1007/s10498-011-9136-1
3. Beinart RA, Gartman A, Sanders JG *et al.* The uptake and excretion of partially oxidized sulfur expands the repertoire of energy resources metabolized by hydrothermal vent symbioses. *Proc Biol Sci* 2015;**282**:20142811. https://doi.org/10.1098/rspb.2014.2811
4. McCollom TM, Shock EL. Geochemical constraints on chemolithoautotrophic metabolism by microorganisms in seafloor hydrothermal systems. *Geochim Cosmochim Acta* 1997;**61**:4375–91. https://doi.org/10.1016/S0016-7037(97)00241-X
5. Hansen M, Perner M. A novel hydrogen oxidizer amidst the sulfur-oxidizing *Thiomicrospira* lineage. *ISME J* 2015;**9**:696–707. https://doi.org/10.1038/ismej.2014.173

6. Böhnke S, Sass K, Gonnella G *et al.* Parameters governing the community structure and element turnover in Kermadec volcanic ash and hydrothermal fluids as monitored by inorganic electron donor consumption, autotrophic CO_2 fixation and 16S tags of the transcriptome in incubation experiments. *Front Microbiol* 2019;**10**:2296. https://doi.org/10.3389/fmicb.2019.02296
7. Ruby EG, Jannasch HW. Physiological characteristics of *Thiomicrospira* sp. strain L-12 isolated from deep-sea hydrothermal vents. *J Bacteriol* 1982;**149**:161–5. https://doi.org/10.1128/jb.149.1.161-165.1982
8. Jannasch HW, Wirsen CO, Nelson DC *et al.* *Thiomicrospira crunogena* sp. nov., a colorless, sulfur-oxidizing bacterium from a deep-sea hydrothermal vent. *Int J Syst Bacteriol* 1985;**35**:422–4. https://doi.org/10.1099/00207713-35-4-422
9. Cao H, Wang Y, Lee OO *et al.* Microbial sulfur cycle in two hydrothermal chimneys on the southwest Indian ridge. *MBio* 2014;**5**:10–1128. https://doi.org/10.1128/mBio.00980-13
10. Ruby EG, Wirsen CO, Jannasch HW. Chemolithotrophic sulfur-oxidizing bacteria from the Galapagos rift hydrothermal vents. *Appl Environ Microbiol* 1981;**42**:317–24. https://doi.org/10.1128/aem.42.2.317-324.1981
11. Brinkhoff T, Muyzer G. Increased species diversity and extended habitat range of sulfur-oxidizing *Thiomicrospira* spp. *Appl Environ Microbiol* 1997;**63**:3789–96. https://doi.org/10.1128/aem.63.10.3789-3796.1997
12. Takai K, Nealson KH, Horikoshi K. Hydrogenimonas thermophila gen. Nov., sp. nov., a novel thermophilic, hydrogen-oxidizing chemolithoautotroph within the ε-Proteobacteria, isolated from a black smoker in a central Indian ridge hydrothermal field. *Int J Syst Evol Microbiol* 2004;**54**:25–32. https://doi.org/10.1099/ijs.0.02787-0
13. Boden R, Scott KM, Williams J *et al.* An evaluation *of Thiomicrospira, Hydrogenovibrio* and *Thioalkalimicrobium*: reclassification of four species of *Thiomicrospira* to each *Thiomicrorhabdus* gen. Nov. and *Hydrogenovibrio*, and reclassification of all four species of *Thioalkalimicrobium* to *Thiomicrospira*. *Int J Syst Evol Microbiol* 2017;**67**:1140–51. https://doi.org/10.1099/ijsem.0.001855
14. Jiang L, Lyu J, Shao Z. Sulfur metabolism of *Hydrogenovibrio thermophilus* strain S5 and its adaptations to deep-sea hydrothermal vent environment. *Front Microbiol* 2017;**8**:1–12. https://doi.org/10.3389/fmicb.2017.02513
15. Barco RA, Hoffman CL, Ramírez GA *et al.* *In-situ* incubation of iron-sulfur mineral reveals a diverse chemolithoautotrophic community and a new biogeochemical role for *Thiomicrospira*. *Environ Microbiol* 2017;**19**:1322–37. https://doi.org/10.1111/1462-2920.13666
16. Brazelton WJ, Baross JA. Metagenomic comparison of two *Thiomicrospira* lineages inhabiting contrasting deep-sea hydrothermal environments. *PLoS One* 2010;**5**:e13530. https://doi.org/10.1371/journal.pone.0013530
17. Adam-Beyer N, Laufer-Meiser K, Fuchs S *et al.* Microbial ecosystem assessment and hydrogen oxidation potential of newly discovered vent systems from the central and south-east Indian ridge. *Front Microbiol* 2023;**14**:1173613. https://doi.org/10.3389/fmicb.2023.1173613
18. Laufer K, Nordhoff M, Røy H *et al.* Coexistence of microaerophilic, nitrate-reducing, and phototrophic Fe(II) oxidizers and Fe(III) reducers in coastal marine sediment. *Appl Environ Microbiol* 2016;**82**:1433–47. https://doi.org/10.1128/AEM.03527-15
19. Lane DJ. 16S/23S rRNA sequencing. In: Stackebrandt E.G., Goodfellow M. (eds.), *Nucleic Acid Techniques Inbacterial Systematics*. Hoboken: John Wiley and Sons, 1991, 115–75.
20. Kumar S, Stecher G, Li M *et al.* MEGA X: molecular evolutionary genetics analysis across computing platforms. *Mol Biol Evol* 2018;**35**:1547–9. https://doi.org/10.1093/molbev/msy096
21. Thompson JD, Higgins DG, Gibson TJ. CLUSTAL W: improving the sensitivity of progressive multiple sequence alignment through sequence weighting, position-specific gap penalties and weight matrix choice. *Nucleic Acids Res* 1994;**22**:4673–80. https://doi.org/10.1093/nar/22.22.4673
22. Emerson D, Moyer C. Isolation and characterization of novel iron-oxidizing bacteria that grow at circumneutral pH. *Environ Microbiol* 1997;**63**:4784–92. https://doi.org/10.1128/aem.63.12.4784-4792.1997
23. Emerson D, Floyd MM. Enrichment and isolation of iron-oxidizing bacteria at neutral pH. *Methods Enzymol* 2005;**397**:112–23. https://doi.org/10.1016/S0076-6879(05)97006-7
24. Stookey LL. Ferrozine-a new spectrophotometric reagent for iron. *Anal Chem* 1970;**42**:779–81. https://doi.org/10.1021/ac60289a016
25. Steudel R, Holdt G, Göbel T *et al.* Chromatographic separation of higher polythionates SnO (n = 3 . . . 22) and their detection in cultures of *Thiobacillus ferroxidans*; molecular composition of bacterial sulfur secretions. *Angew Chemie Int Ed English* 1987;**26**:151–3. https://doi.org/10.1002/anie.198701511
26. Schippers A, Jørgensen BB. Oxidation of pyrite and iron sulfide by manganese dioxide in marine sediments. *Geochim Cosmochim Acta* 2001;**65**:915–22. https://doi.org/10.1016/S0016-7037(00)00589-5
27. Laufer K, Røy H, Jørgensen BB *et al.* Evidence for the existence of autotrophic nitrate-reducing Fe(II)-oxidizing bacteria in marine coastal sediment. *Appl Env Microbiol* 2016;**82**:6120–31. https://doi.org/10.1128/AEM.01570-16
28. Böhnke S, Perner M. A function-based screen for seeking RubisCO active clones from metagenomes: novel enzymes influencing RubisCO activity. *ISME J* 2015;**9**:735–45. https://doi.org/10.1038/ismej.2014.163
29. Jakob R, Saenger W. Reversed-phase ion-pair chromatographic separation of ribulose 1,5-bisphosphate from 3-phosphoglycerate and its application as a new enzyme assay for RuBP carboxylase/oxygenase. *FEBS Lett* 1985;**183**:111–4. https://doi.org/10.1016/0014-5793(85)80965-0
30. Garber AI, Nealson KH, Okamoto A *et al.* FeGenie: a comprehensive tool for the identification of iron genes and iron gene neighborhoods in genome and metagenome assemblies. *Front Microbiol* 2020;**11**:499513. https://doi.org/10.3389/fmicb.2020.00037
31. Perner M, Hentscher M, Rychlik N *et al.* Driving forces behind the biotope structures in two low-temperature hydrothermal venting sites on the southern mid-Atlantic ridge. *Environ Microbiol Rep* 2011;**3**:727–37. https://doi.org/10.1111/j.1758-2229.2011.00291.x
32. Perner M, Hansen M, Seifert R *et al.* Linking geology, fluid chemistry, and microbial activity of basalt-and ultramafic-hosted deep-sea hydrothermal vent environments. *Geobiology* 2013;**11**:340–55. https://doi.org/10.1111/gbi.12039
33. Toyoda K, Ishii M, Arai H. Function of three RuBisCO enzymes under different CO_2 conditions in *Hydrogenovibrio marinus*. *JBiosci Bioeng* 2018;**126**:730–5. https://doi.org/10.1016/j.jbiosc.2018.06.005
34. Moeck GS, Coulton JW. TonB-dependent iron acquisition: mechanisms of siderophore-mediated active transport. *Mol Microbiol* 1998;**28**:675–81. https://doi.org/10.1046/j.1365-2958.1998.00817.x

35. Ferguson AD, Deisenhofer J. TonB-dependent receptors—structural perspectives. *Biochim Biophys Acta Biomembr* 2002; **1565**:318–32. https://doi.org/10.1016/S0005-2736(02)00578-3
36. Ringel MT, Brüser T. The biosynthesis of pyoverdines. Microb. *Cell* 2018;**5**:424–37. https://doi.org/10.15698/mic2018.10.649
37. Scott KM, Sievert SM, Abril FN *et al.* The genome of deep-sea vent chemolithoautotroph *Thiomicrospira crunogena* XCL-2. *PLoS Biol* 2006;**4**:2196–212. https://doi.org/10.1371/journal.pbio.0040383
38. Hansen M, Perner M. Hydrogenase gene distribution and H_2 consumption ability within the *Thiomicrospira* lineage. *Front Microbiol* 2016;**7**:99. https://doi.org/10.3389/fmicb.2016.00099
39. Frigaard NU, Bryant DA. Genomic insights into the sulfur metabolism of phototrophic green sulfur bacteria. In: Hell R., Dahl C., Knaff D. *et al.* (eds.), *Sulfur Metabolism in Phototrophic Organisms*. Dordrecht: Springer, 2008, 337–55 10.1007/978-1-4020-6863-8_17.
40. Gregersen LH, Bryant DA, Frigaard NU. Mechanisms and evolution of oxidative sulfur metabolism in green sulfur bacteria. *Front Microbiol* 2011;**2**:116. https://doi.org/10.3389/fmicb.2011.00116
41. Scott KM, Williams J, Porter CM *et al.* Genomes of ubiquitous marine and hypersaline *Hydrogenovibrio, Thiomicrorhabdus* and *Thiomicrospira* spp. encode a diversity of mechanisms to sustain chemolithoautotrophy in heterogeneous environments. *Environ Microbiol* 2018;**20**:2686–708. https://doi.org/10.1111/1462-2920.14090
42. Erb TJ, Zarzycki J. A short history of RubisCO: the rise and fall (?) of Nature's predominant CO_2 fixing enzyme. *Curr Opin Biotechnol* 2018;**49**:100–7. https://doi.org/10.1016/j.copbio.2017.07.017
43. Yoichi Y, Koichi T, Hiroyuki A *et al.* CO_2-responsive expression and gene organization of three ribulose-1,5-bisphosphate carboxylase/oxygenase enzymes and carboxysomes in *Hydrogenovibrio marinus* strain MH-110. *J Bacteriol* 2004;**186**:5685–91. https://doi.org/10.1128/JB.186.17.5685-5691.2004
44. Scott KM, Leonard JM, Boden R *et al.* Diversity in CO_2-concentrating mechanisms among chemolithoautotrophs from the genera *Hydrogenovibrio, Thiomicrorhabdus*, and *Thiomicrospira,* ubiquitous in sulfidic habitats worldwide. *Appl Environ Microbiol* 2019;**85**:e02096–18. https://doi.org/10.1128/AEM.02096-18
45. Dobrinski KP, Longo DL, Scott KM. The carbon-concentrating mechanism of the hydrothermal vent chemolithoautotroph *Thiomicrospira crunogena*. *J Bacteriol* 2005;**187**:5761–6. https://doi.org/10.1128/JB.187.16.5761-5766.2005
46. Adam N, Han Y, Laufer-Meiser K *et al.* Deltaproteobacterium strain KaireiS1, a mesophilic, hydrogen-oxidizing and sulfate-reducing bacterium from an inactive deep-sea hydrothermal chimney. *Front Microbiol* 2021;**12**:686276. https://doi.org/10.3389/fmicb.2021.686276
47. Qin H, Guan X, Bandstra JZ *et al.* Modeling the kinetics of hydrogen formation by zerovalent iron: effects of sulfidation on micro- and nano-scale particles. *Environ Sci Technol* 2018;**52**:13887–96. https://doi.org/10.1021/acs.est.8b04436
48. Mori JF, Scott JJ, Hager KW *et al.* Physiological and ecological implications of an iron- or hydrogen-oxidizing member of the Zetaproteobacteria, *Ghiorsea bivora*, gen. Nov., sp. nov. *ISME J* 2017;**11**:2624. https://doi.org/10.1038/ismej.2017.132
49. Emerson D, Rentz JA, Lilburn TG *et al.* A novel lineage of proteobacteria involved in formation of marine Fe-oxidizing microbial mat communities. *PLoS One* 2007;**2**:e667. https://doi.org/10.1371/journal.pone.0000667
50. McAllister SM, Moore RM, Gartman A *et al.* The Fe(II)-oxidizing Zetaproteobacteria: historical, ecological and genomic perspectives. *FEMS Microbiol Ecol* 2019;**95**:fiz015. https://doi.org/10.1093/femsec/fiz015
51. Hribovšek P, Olesin Denny E, Dahle H *et al.* Putative novel hydrogen-and iron-oxidizing sheath-producing Zetaproteobacteria thrive at the Fåvne deep-sea hydrothermal vent field. *Msyst* 2023;**8**:e00543–23. https://doi.org/10.1128/msystems.00543-23
52. Baker IR, Matzen SL, Schuler CJ *et al.* Aerobic iron-oxidizing bacteria secrete metabolites that markedly impede abiotic iron oxidation. *PNAS nexus* 2023;**2**:pgad421. https://doi.org/10.1093/pnasnexus/pgad421
53. Neely C, Bou Khalil C, Cervantes A *et al.* Genome sequence of *Hydrogenovibrio* sp. strain SC-1, a chemolithoautotrophic sulfur and iron oxidizer. *Genome Announc* 2018;**6**:4–5. https://doi.org/10.1128/genomeA.01581-17
54. Hoffman CL, Monreal PJ, Albers JB *et al.* Microbial strong organic ligand production is tightly coupled to iron in hydrothermal plumes. *bioRxiv* 2023; 2023.01.05.522639. https://doi.org/10.1101/2023.01.05.522639
55. Gledhill M, Buck KN. The organic complexation of iron in the marine environment: a review. *Front Microbiol* 2012;**3**:69. https://doi.org/10.3389/fmicb.2012.00069
56. Noinaj N, Guillier M, Barnard TJ *et al.* TonB-dependent transporters: regulation, structure, and function. *Ann Rev Microbiol* 2010;**64**:43–60. https://doi.org/10.1146/annurev.micro.112408.134247
57. Ziervogel K, Arnosti C. Substantial carbohydrate hydrolase activities in the water column of the Guaymas Basin (gulf of California). *Front Mar Sci* 2020;**6**:815. https://doi.org/10.3389/fmars.2019.00815
58. Li M, Toner BM, Baker BJ *et al.* Microbial iron uptake as a mechanism for dispersing iron from deep-sea hydrothermal vents. *Nat Commun* 2014;**5**:3192. https://doi.org/10.1038/ncomms4192
59. Amend JP, Shock EL. Energetics of overall metabolic reactions of thermophilic and hyperthermophilic archaea and bacteria. *FEMS Microbiol Rev* 2001;**25**:175–243. https://doi.org/10.1111/j.1574-6976.2001.tb00576.x
60. Fuchs G. *Allgemeine Mikrobiologie*, 11th edn. Stuttgart: Georg Thieme Verlag, 2007, 10.1055/b-002-44938.
61. Emerson D, Fleming EJ, McBeth JM. Iron-oxidizing bacteria: an environmental and genomic perspective. *Ann Rev Microbiol* 2010;**64**:561–83. https://doi.org/10.1146/annurev.micro.112408.134208
62. Boschker HTS, Vasquez-Cardenas D, Bolhuis H *et al.* Chemoautotrophic carbon fixation rates and active bacterial communities in intertidal marine sediments. *PLoS One* 2014;**9**:e101443. https://doi.org/10.1371/journal.pone.0101443
63. Jørgensen BB, Nelson DC. Sulfide oxidation in marine sediments: geochemistry meets microbiology. *Geol Soc Am Spec Pap* 2004;**379**:63–81. https://doi.org/10.1130/0-8137-2379-5.63
64. Howarth RW, Jørgensen BB. Formation of ^{35}S-labelled elemental sulfur and pyrite in coastal marine sediments (Limfjorden and Kysing Fjord, Denmark) during short-term $^{35}SO_4^{2-}$ reduction measurements. *Geochim Cosmochim Acta* 1984;**48**:1807–18. https://doi.org/10.1016/0016-7037(84)90034-6
65. Thomsen U, Kristensen E. Dynamics of ΣCO_2 in a surficial sandy marine sediment: the role of chemoautotrophy. *Aquat Microb Ecol* 1997;**12**:165–76. https://doi.org/10.3354/ame012165
66. Wuchter C, Abbas B, Coolen MJ *et al.* Archaeal nitrification in the ocean. *Proc Natl Acad Sci* 2006;**103**:12317–22. https://doi.org/10.1073/pnas.0600756103
67. Berg C, Listmann L, Vandieken V *et al.* Chemoautotrophic growth of ammonia-oxidizing Thaumarchaeota enriched from a pelagic redox gradient in the Baltic Sea. *Front Microbiol* 2014;**5**:786.
68. Billen G. Evaluation of nitrifying activity in sediments by dark ^{14}C-bicarbonate incorporation. *Water Res* 1976;**10**:51–7. https://doi.org/10.1016/0043-1354(76)90157-3

69. Kelly DP. Biochemistry of the chemolithotrophic oxidation of inorganic Sulphur. *Philos Trans R Soc Lond Biol Sci* 1982;**298**:499–528. https://doi.org/10.1098/rstb.1982.0094
70. Timmer-ten HA. Cell yield and bioenergetics of *Thiomicrospira denitrificans* compared with *Thiobacillus denitrificans*. *Antonie Van Leeuwenhoek* 1981;**47**:231–43. https://doi.org/10.1007/BF00403394
71. Nelson DC, Jørgensen BB, Revsbech NP. Growth pattern and yield of a chemoautotrophic Beggiatoa sp. in oxygen-sulfide microgradients. *Appl Env Microbiol* 1986;**52**:225–33. https://doi.org/10.1128/aem.52.2.225-233.1986
72. Neubauer SC, Emerson D, Megonigal JP. Life at the energetic edge: kinetics of circumneutral iron oxidation by lithotrophic iron-oxidizing bacteria isolated from the wetland-plant rhizosphere. *Appl Env Microbiol* 2002;**68**:3988–95. https://doi.org/10.1128/AEM.68.8.3988-3995.2002
73. Sobolev D, Roden EE. Characterization of a neutrophilic, chemolithoautotrophic Fe(II)-oxidizing β-Proteobacterium from freshwater wetland sediments. *Geomicrobiol J* 2004;**21**:1–10. https://doi.org/10.1080/01490450490253310
74. Sarrazin J, Rodier P, Tivey MK *et al.* A dual sensor device to estimate fluid flow velocity at diffuse hydrothermal vents. *Deep Sea Res Part I Oceanogr Res Pap* 2009;**56**:2065–74. https://doi.org/10.1016/j.dsr.2009.06.008
75. Wankel SD, Germanovich LN, Lilley MD *et al.* Influence of subsurface biosphere on geochemical fluxes from diffuse hydrothermal fluids. *Nat Geosci* 2011;**4**:461–8. https://doi.org/10.1038/ngeo1183
76. Takai K, Campbell BJ, Cary SC *et al.* Enzymatic and genetic characterization of carbon and energy metabolisms by deep-sea hydrothermal chemolithoautotrophic isolates of *Epsilonproteobacteria*. *Appl Environ Microbiol* 2005;**71**:7310–20. https://doi.org/10.1128/AEM.71.11.7310-7320.2005